Supplementary Information

# Role of the Fe-$FeCl_2$ Contact Interface in Promoting Redox Reversibility and Electrochemical Kinetics in Fe/$FeCl_2$-Graphite Molten Salt Battery

*Wenlong Zhang, Xiaohui Ning**

**Author Address**

*Wenlong Zhang*-Center for Alloy Innovation and Design (CAID), State Key Laboratory for Mechanical Behavior of Materials, Xi'an Jiaotong University, Xi'an, Shaanxi 710049, P. R. China.

*Xiaohui Ning*-Center for Alloy Innovation and Design (CAID), State Key Laboratory for Mechanical Behavior of Materials, Xi'an Jiaotong University, Xi'an, Shaanxi 710049, P. R. China. Email: xiaohuining@mail.xjtu.edu.cn

Number of pages: 10

Number of figures: 18

# Table of Contents

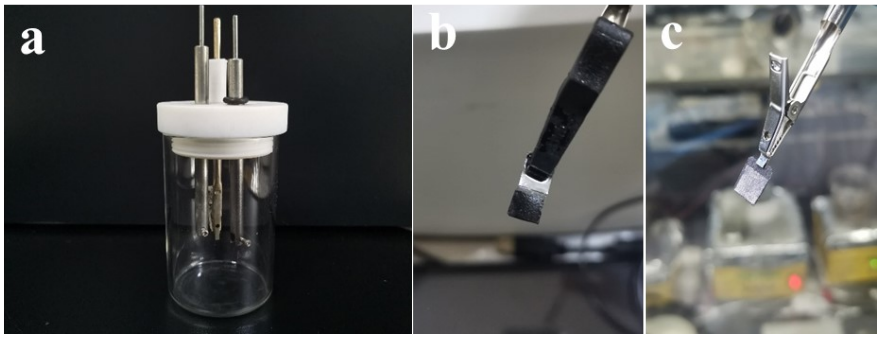


**Figure S1.** (a) Schematic diagram of three-electrode testing device. (b)The $FeCl_2$-CR electrode prepared by powder calendaring. (c) The graphite electrode clamped by molybdenum mesh.

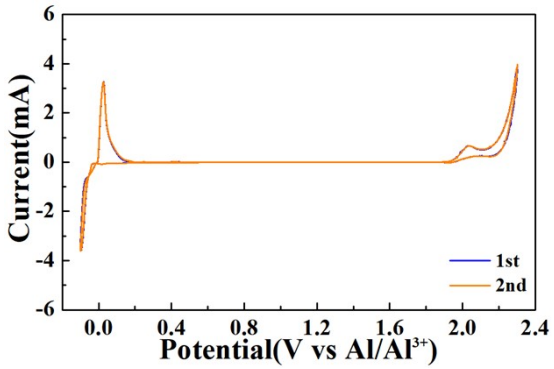


**Figure S2.** CV Curves of the Au electrode in three-electrode system at 10 mV/s.

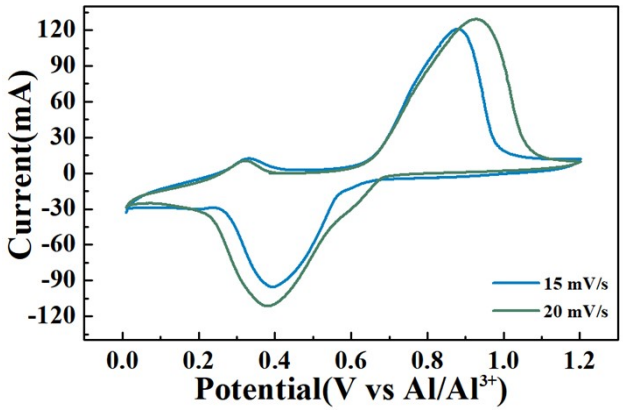


**Figure S3.** CV Curves of the Fe-$FeCl_2$-CR-60 electrode in three-electrode system at 15 mV/s and 20 mV/s.

.

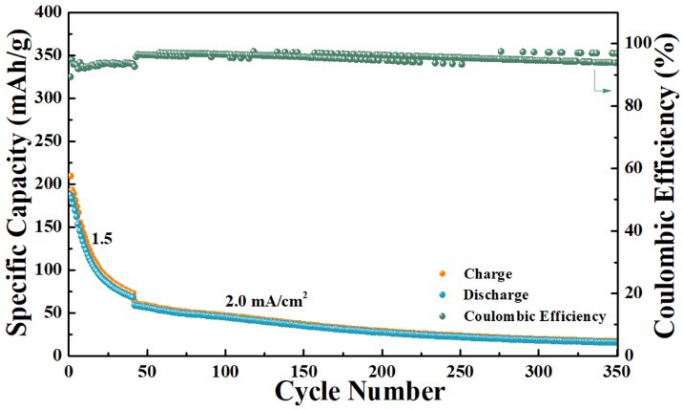


**Figure S4.** Cycling performance of the $FeCl_2$-CR electrode in Fe/$FeCl_2$-Graphite molten salt battery.

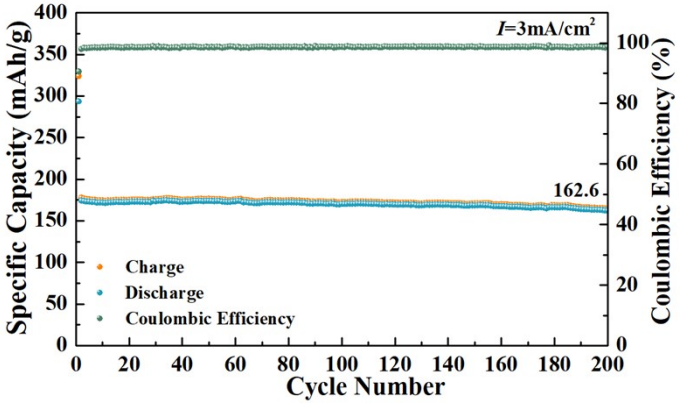


**Figure S5.** Cycling performance of the Fe-$FeCl_2$-CR-60 electrode in Fe/$FeCl_2$-Graphite molten salt battery.

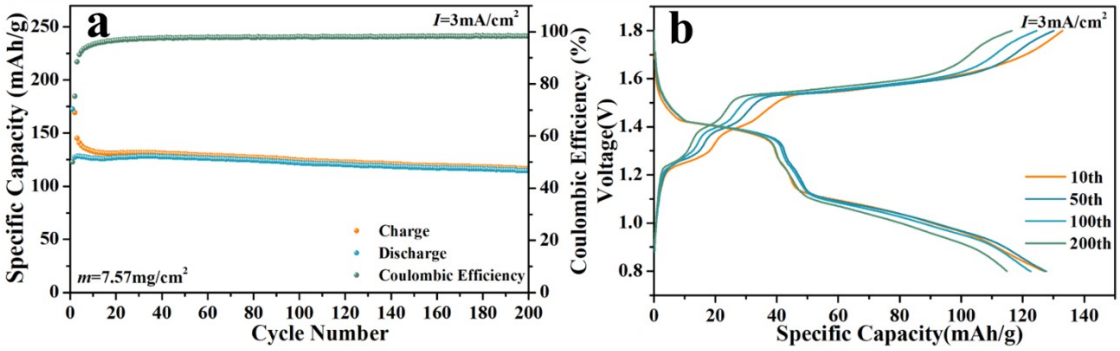


**Figure S6.** (a) Cycling performance of the Fe-$FeCl_2$-CR-60 electrode with enhanced mass loading in Fe/$FeCl_2$-graphite molten salt battery. (b) The corresponding voltage curves of the Fe-$FeCl_2$-CR-60 electrode with enhanced mass loading.

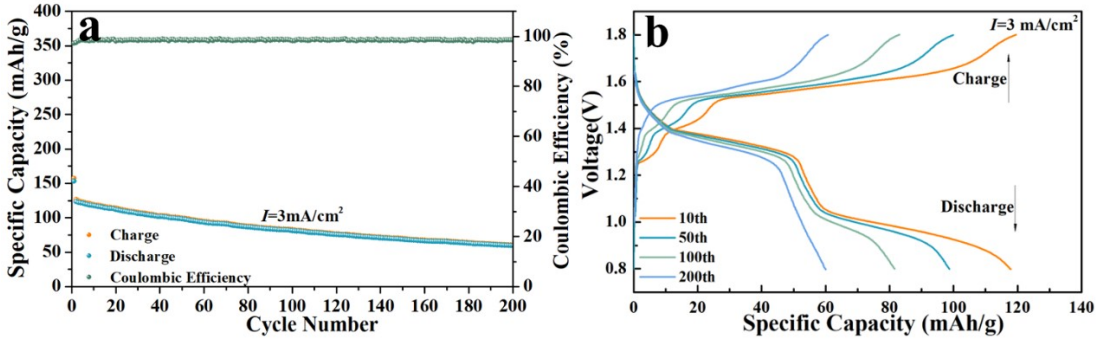


**Figure S7.** (a) Cycling performance of the Fe-$FeCl_2$-CR-20 electrode in Fe/$FeCl_2$-Graphite molten salt battery. (b) The corresponding voltage curves of the Fe-$FeCl_2$-CR-20 electrode.

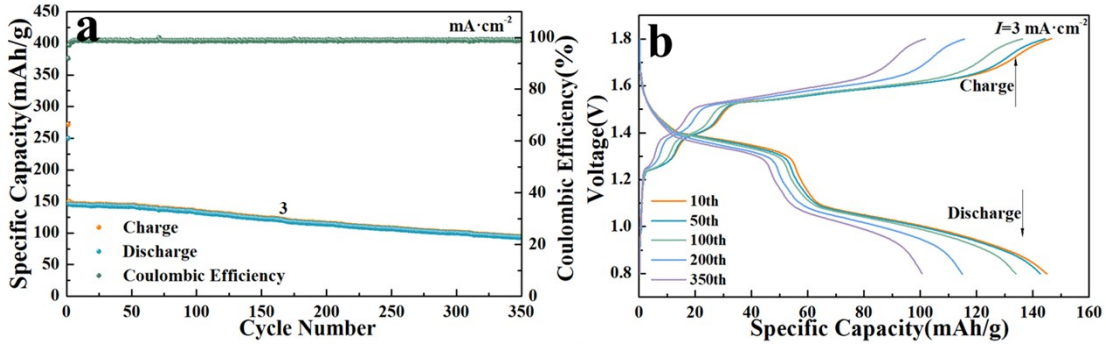

**Figure S8.** (a) Cycling performance of the Fe-$FeCl_2$-CR-40 electrode in Fe/$FeCl_2$-Graphite molten salt battery. (b) The corresponding voltage curves of the Fe-$FeCl_2$-CR-40 electrode.

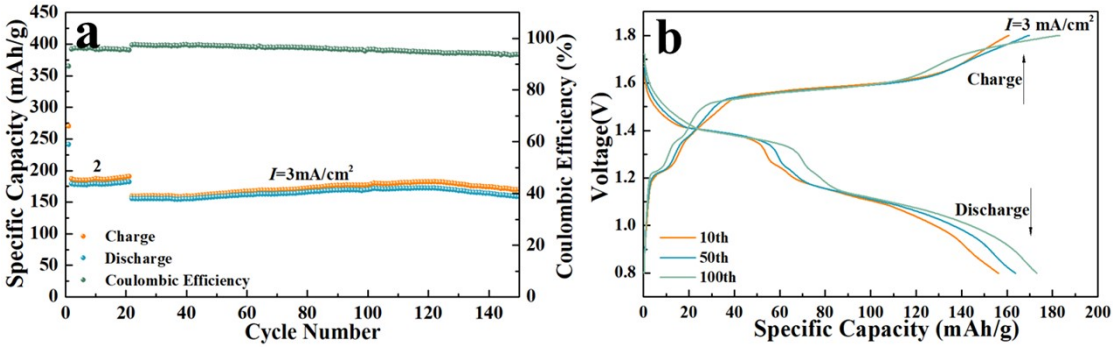


**Figure S9.** (a) Cycling performance of the Fe-$FeCl_2$-CR-80 electrode in Fe/$FeCl_2$-Graphite molten salt battery. (b) The corresponding voltage curves of the Fe-$FeCl_2$-CR-80 electrode.

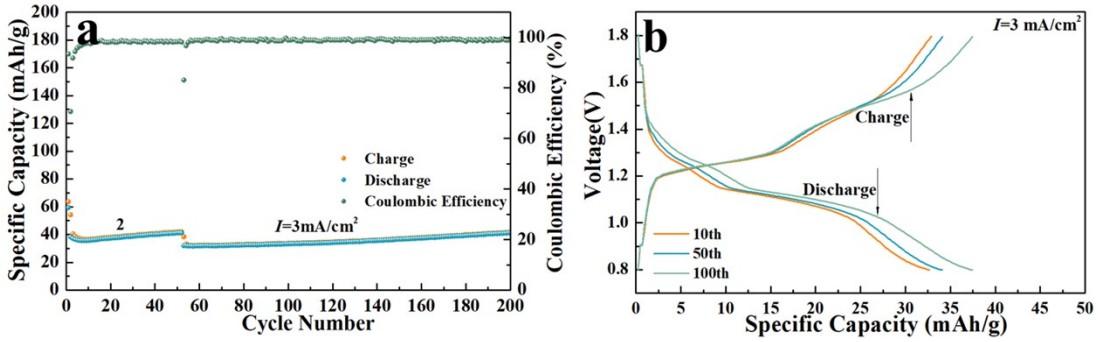


**Figure S10.** (a) Cycling performance of the Fe-CR electrode in Fe/$FeCl_2$-Graphite molten salt battery. (b) The corresponding voltage curves of the Fe-CR electrode.

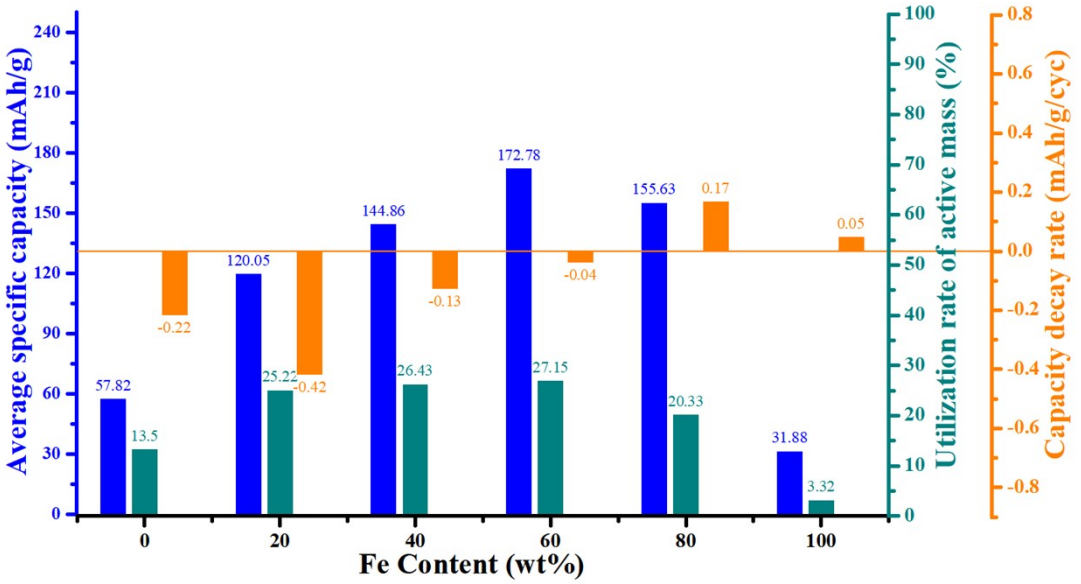


**Figure S11.** The electrochemical characteristics of Fe-$FeCl_2$-CR electrodes with different Fe contents.

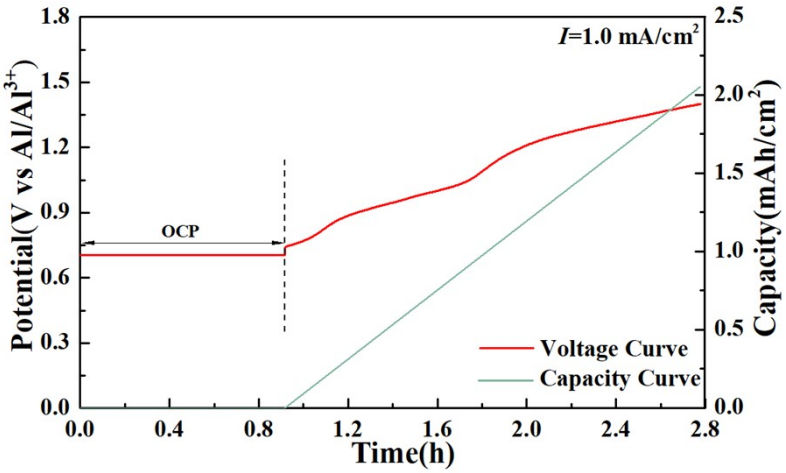


**Figure S12.** Galvanostatic chlorination curves of Fe-CR electrode.

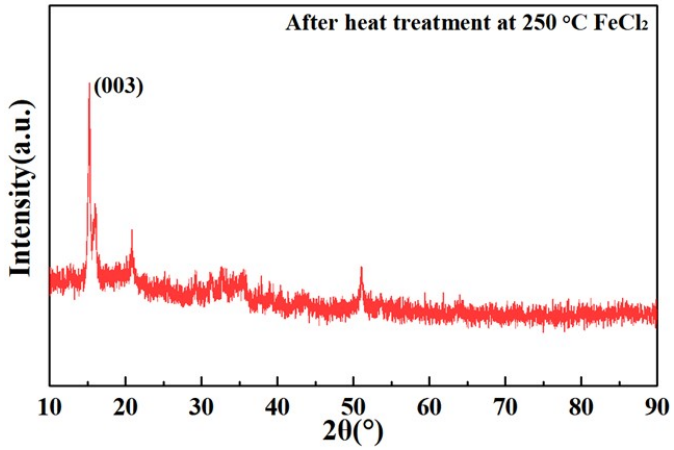


**Figure S13.** XRD pattern of $FeCl_2$ material.

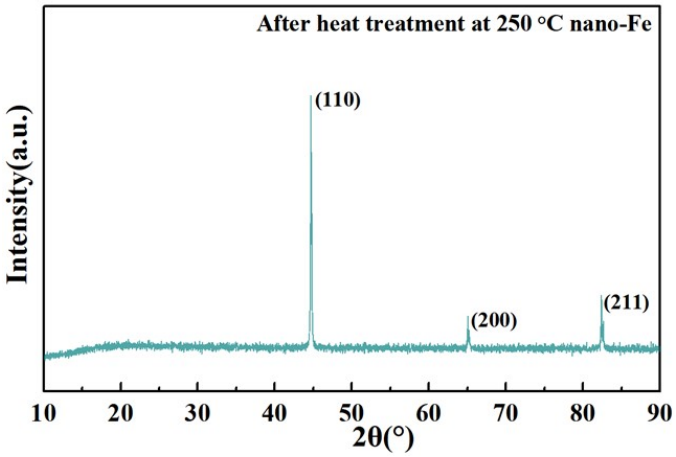


**Figure S14.** XRD pattern of nano-Fe powder material.

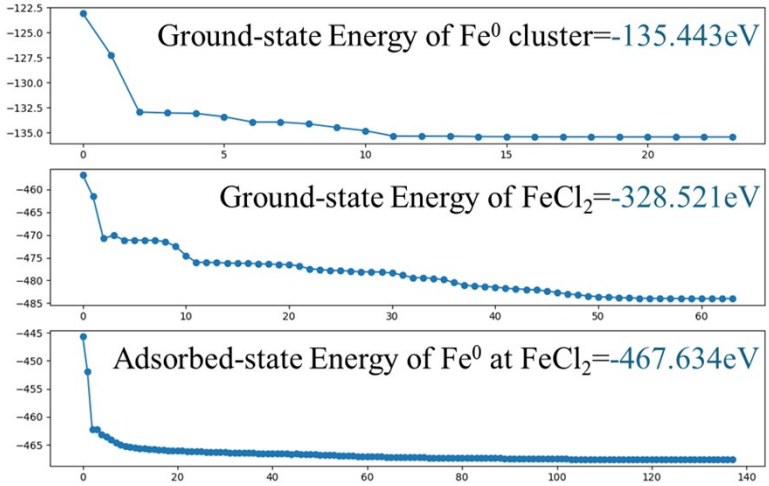


**Figure S15.** The original chart of the adsorbed energy calculation (-3.67eV) of $Fe^0$ cluster at $FeCl_2$ (003).

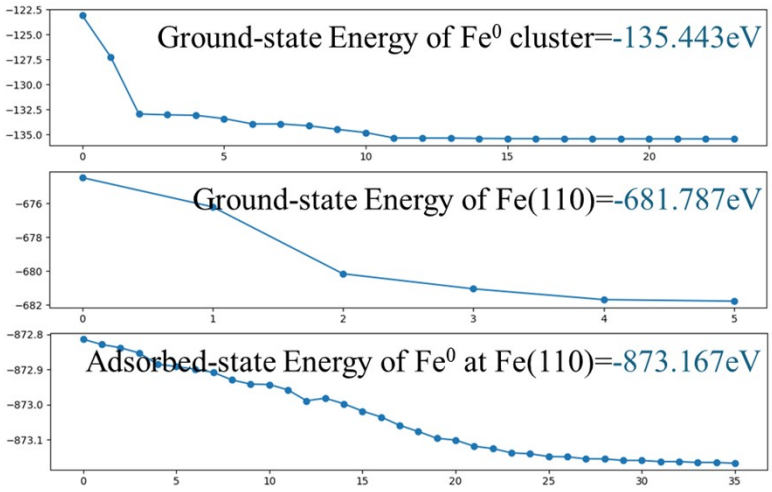


**Figure S16.** The original chart of the adsorbed energy calculation (-55.937eV) of $Fe^0$ cluster at Fe (110).

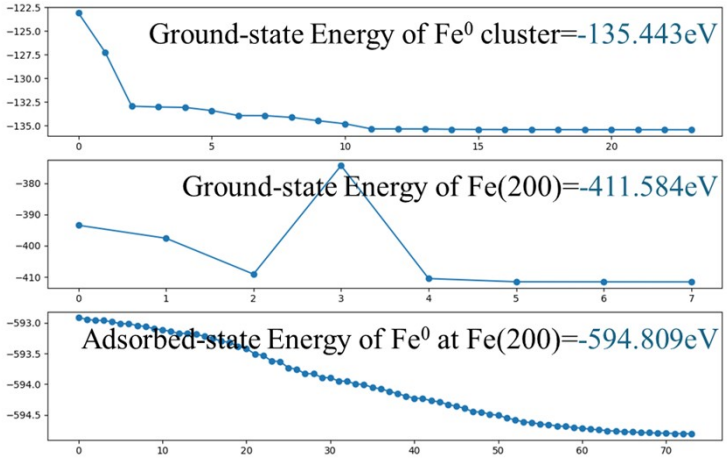


**Figure S17.** The original chart of the adsorbed energy calculation (-47.782eV) of $Fe^0$ cluster at Fe (200).

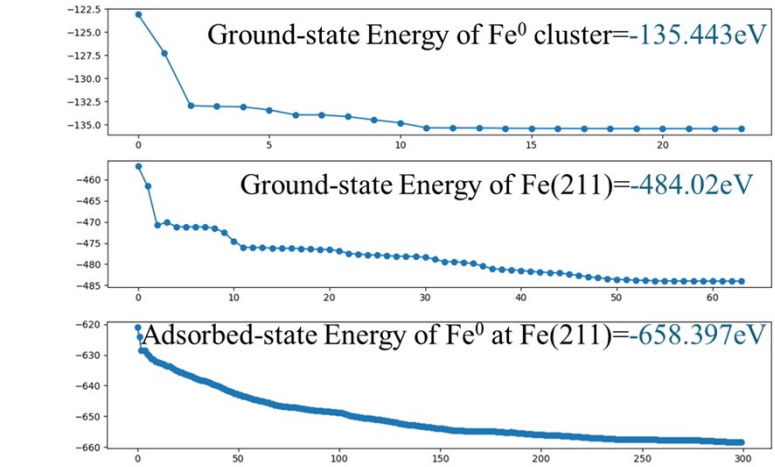


**Figure S18.** The original chart of the adsorbed energy calculation (-38.934eV) of $Fe^0$ cluster at Fe (211).